Accuracy of the Spider Model in Decomposing Layered Surfaces

Tetsuro Morimoto
Toppan Printing Co. Ltd.
Japan
tetsuro.morimoto@toppan.co.jp

Robby T. Tan
Utrecht University
The Netherlands
tanrobby@gmail.com

Rei Kawakami
The University of Tokyo
Japan
rei@cvl.iis.u-tokyo.ac.jp

Katsushi Ikeuchi
The University of Tokyo
Japan
ki@cvl.iis.u-tokyo.ac.jp

Abstract

The surface of most natural objects is composed of two or more layers whose optical properties jointly determine the surface's overall reflectance. Light transmission through these layers can be approximated by using the Lambert-Beer (LB) model, which provides a good trade-off between the accuracy and simplicity to handle layer decomposition. Recently, a layer decomposition based on the LB-based model is proposed. Assuming surfaces with two layers, it estimates the reflectance of top and bottom layers, as well as the opacity of the top layer. The method introduces the "spider model", which is named after the color distribution in the RGB space that resembles the shape of spiders. In this paper, we intend to verify the accuracy of the spider model and the optical model where it is based on (i.e., the LB-based model). We verify the LB-based model by comparing to the Kubelka-Munk (KM) model, which has previously been shown to be reliably accurate. The benefits of layer decomposition are easy to notice. First, many computer vision algorithms assume a single layer, and tend to fail when encountering multi-layered surfaces. Second, knowing the optical properties of each layer can provide further knowledge of the target objects.

1. Introduction

In computer vision, reflectance is conventionally assumed to follow a single-layer reflection model, such as the Lambertian model [16]. While this model can serve as an approximation of reflection of a single-layered surface, most objects in the real world, particularly natural ones, have surfaces that consist of multiple layers. For such objects, single layer models often provide a poor representation of their reflectance characteristics.

In multi-layered surfaces, each layer may have different optical parameter values. These values and the order of the layers physically determine the reflectance of an object, and therefore also the object's appearance. For example, human skin roughly consists of two layers, namely the dermis and epidermis [1], which both contribute to the unique appearance of skin. Other examples are plant leaves, biological tissues, and oxidized metals (patinas), paintings, etc.

Decomposing such surfaces, which means extracting each layer optical properties, can benefit computer vision applications and other fields, such as archeology, biology, medical image analysis, etc. Morimoto et al. [18] proposed a novel method that can extract the optical properties of layered surfaces with two layers (i.e., top and bottom layers). The method extracts the opacity of the top layer and the reflection of both layers using the spider model. Given a single input image containing one bottom layer and at least one top layer, it fits the color distributions in the RGB space using the spider model, and then estimates the optical parameters.

The spider model proposed in [18] is a nonlinear equation describing the correlation of the intensity values of layered surfaces in the RGB space. It is called spider model since, when the intensity values of the mixtures of one bottom layer and n different top layers are projected onto the color space, then we will have n different curves intersecting at one point, resembling the shape of a spider. As discussed in [18], the core of the spider model is the Lambert-Beer (LB) based model.

However, to our best knowledge, there are no discussion in the literature about the accuracy of the LB-based model applied to layered surfaces and thus the spider model. Therefore, in this paper, our goal is to verify the accuracy of the two models. For verifying the LB-based model, we will compare it with the Kubelka-Munk (KM) model, a two-flux scattering model; while for the spider model, we will investigate the differences of its generated RGB values from the color distributions of real data.

The fields of optics and color science have introduced many models of multi-layered objects [5, 13]. These models are principally based on radiative transfer theory [6]. One highly detailed representation is the many-flux scattering model presented by Mudgett *et al*. [19]. Since this model has many parameters that make it difficult to apply, a simpler two-flux approximation called the Kubelka-Munk (KM) model [15] is practically more useful, particularly in color science. Mudgett *et al*. [20] has theoretically verified that the KM model works reliably (when the scattering coefficient is relatively higher than the absorption coefficient); which is the main reason for us to use it as the standard for the verification. Note that, while the KM model (which is a two-flux model) is considerably simpler than multi-flux models, in computer vision, the model is still considerably complex, due to the highly nonlinear equation.

The KM model has been used to heighten the realism of pigmented materials [11] and weathered objects [10]. It has been frequently used in color matching of textiles, paints, printing inks and plastics (e.g., [9, 4]). Tsumura *et al*. [22] decomposed melanin and hemoglobin of human skin based on the Lambert-Beer (LB) law [2] and later used the model to generate skin colors under various values of melanin and hemoglobin concentrations [23]. Some researchers have employed the alpha matting equation for decomposing layered scenes (e.g., [7, 17]). Since alpha matting utilizes a linear equation to model layer composition, it can be considered as physically consistent with the LB law [21]. However, most methods using the alpha matting equation assume the opacity to be independent from the wavelengths, which is different from the LB-based model [18]. In terms of the mathematical equation, the LB-based model is identical to Koschmieder's equation for radiance [14]; although to our knowledge, the equation has never been applied to layered surfaces.

Organization The rest of this paper is organized as follows. First, we review the layered surface decomposition using the spider model in Section 2. In Section 3, we discuss the two reflection models: the LB-based model and the KM model, and compare them in Section 4. In Section 5, we provide a discussion about the accuracy and effectiveness of the LB-based model, followed by conclusions in Section 6.

2. Layered Surface Decomposition

Morimoto *et al*. [18] propose a layered-surface decomposition method using the spider model. The method assumes two layers and estimates the following three optical properties: bottom layer's reflection, top layer's reflection and top layer's opacity. An example of their decomposition is shown in Fig. 1, where an ancient wall painting is decomposed into its top and bottom layers, and its opacity. The estimated top layer reveals the painting of the ship, which is faded and harder to see in the original input image.

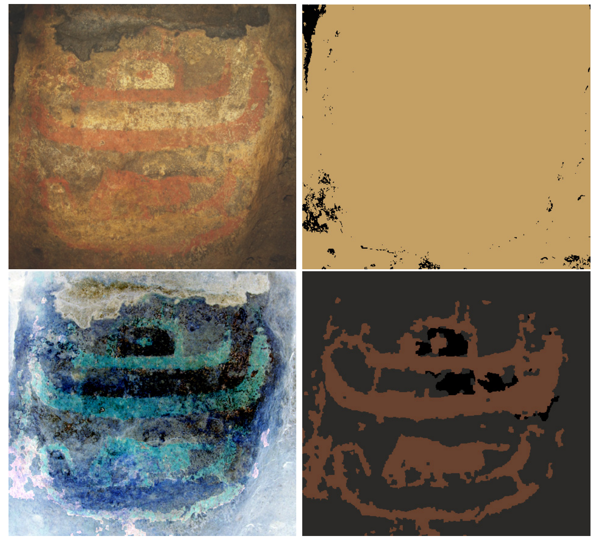

Figure 1. A layered surface decomposition result of wall painting assuming two layers. Top left: input image. Top right: the estimated bottom layer. Bottom left: the estimated opacity. Bottom right: the estimated top layer.

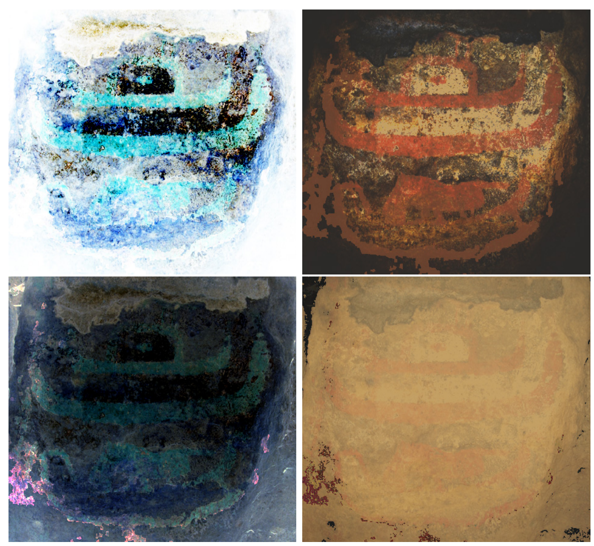

Figure 2. A simulation using the estimated opacity in Fig. 1. Top left: the reduced opacity image. Top right: the simulated appearance with reduced opacity. Bottom left: the enhanced opacity image. Bottom right: the simulated appearance with enhanced opacity.

There are two applications of the layered-surface decomposition. First, the estimated top layer is useful in color seg-

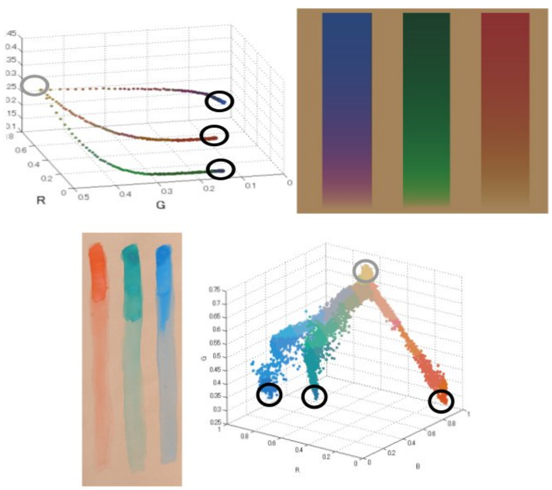

Figure 3. Spider model: Top row. Right: the generated image using LB-based model. Left: we plotted three colors with various opacity values into the RGB space. The gray circle represents the bottom layer's reflection. Black circles represent the top layer's reflection when the opacity=1. Each of the line follows the spider model in Eqs. (1) and (2). Bottom row. Left: the real image. Right: the plot of the left image into the RGB space. The gray circle represents the bottom layer's reflection. Black circles represent the top layer's reflection with the largest opacity value.

mentation which normally suffers from color gradations of top layers. Second, the three estimated properties are useful to simulate the synthetic appearance of a target object. Fig. 2 shows the results of changing the opacity. By either reducing or increasing the opacity, the image can fade out or become more salient.

Spider Model The spider model, which is the core in [18], is based on the Lambert-Beer law [2], and is mathematically described as follows:

$$I_r = B_r + \psi_r (I_g - B_g)^{\gamma_r}, \quad (1)$$
$$I_b = B_b + \psi_b (I_g - B_g)^{\gamma_b}, \quad (2)$$

where I_c is the intensity of the input image (the mixed reflection of layered surfaces), c is the index of the RGB color channels, B_c is the reflection of the bottom layer, F_c is the reflection of the top layer, $\gamma_r = \mu_r/\mu_g$, $\psi_r = (F_r - B_r)/(F_g - B_g)^{\gamma_r}$, $\psi_b = (F_b - B_b)/(F_g - B_g)^{\gamma_b}$, and $\gamma_b = \mu_b/\mu_g$, where μ_c is the attenuation factor of the Lambert-Beer law. Each of the variables is dependent on x, the location of the pixel in the image.

The spider model is named after the shape of the plot of the model in a three-dimensional space (the space is not necessarily composed of the RGB color channels, but any three wavelengths with considerable distance among them). Due to the non-linear correlation between color channels

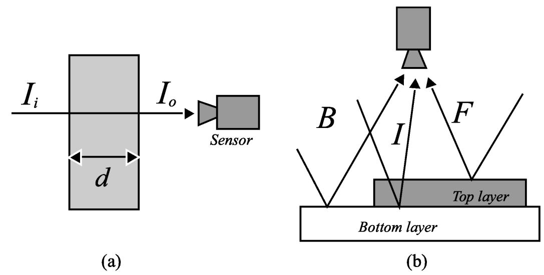

Figure 4. (a).The optical model of the Lambert-beer model. (b).The optical model based on the Lambert-Beer model of layered surface objects

represented in Eqs. (1) and (2), the distribution forms a curve as depicted in Fig. 3. When multiple lines are observed, they resemble the shape of a spider. Each line starts at the color of the top layer with the largest opacity. The opacity decreases along with the line. The end point represents the bottom layer's color where the opacity of the top layer is equal to zero. By fitting the model to the observed data, the optical parameters of the layered surface can be obtained.

3. Reflection Models

3.1. Lambert-Beer based Model

Lambert-Beer Law [2] models the optical transmittance of light passing through a transparent object:

$$T(\lambda) = \frac{I_o(\lambda)}{I_i(\lambda)} = e^{-\mu(\lambda)d}, \quad (3)$$

where T is the optical transmittance, λ is the wavelength, I_o is the intensity of the outgoing light, I_i is the intensity of the incoming light, μ is the attenuation factor of the object, and d is the distance of the light traveling through the object. This law is illustrated in Fig. 4.a.

Based on the Lambert-Beer Law, the light reflected from layered surfaces can be modeled as:

$$I_c(x) = B_c(x) e^{-\mu_c(x)d(x)} + F_c(x)\Big(1 - e^{-\mu_c(x)d(x)}\Big), \quad (4)$$

where index c represents one of the three color channels {r,g,b}. I_c is the mixture intensity of the transmitted light from bottom and top layers. We call I_c a mixed layer. B_c and F_c are, respectively, the bottom and top layer's reflectance, when its thickness d is infinitely large. In this paper, we define opacity $\phi_c = 1 - e^{-\mu_c d}$. Finally, x is the spatial image coordinate, which for the sake of simplicity, we will omit throughout the paper. In the last equation, we assume that the camera's color sensitivities follow the Dirac delta function. Although the model can be applied to spectral data, in this paper we focus on RGB images taken from an ordinary digital camera whose gamma correction is set to off. Fig. 4.b illustrates the model.

Hence, if we have two-layered surfaces, they are composed of the bottom layer B_c, the top layer F_c, and the opacity of the top layer ϕ. In this paper, we assume that the opacity of the bottom layer is infinitely large throughout the input image, and also assume that the light coming on the top layer is the same as that of the bottom layer. Therefore, based on the assumptions, we can calculate the mixed reflectance by canceling the incoming light intensity:

$$R_m = R_b\Big(1-\phi\Big) + R_f\phi, \tag{5}$$

where R_m is the mixed reflectance, R_b is the bottom layer's reflectance, and R_f is the top layer's reflectance.

3.2. Kubelka-Munk Model

In this section, we provide a brief review of the KM model. For complete derivations and further details, readers are referred to [13, 24, 12]. Assuming we have a surface covered by a colorant as shown in Fig. 4.b, according to the KM model we can describe the mixed reflectance R_m of the surface as:

$$R_m = \frac{\frac{1}{R_f}(R_b - R_f) - R_f(R_b - \frac{1}{R_f})e^{Sd(\frac{1}{R_f}-R_f)}}{(R_b - R_f) - (R_b - \frac{1}{R_f})e^{Sd(\frac{1}{R_f}-R_f)}}, \tag{6}$$

where R_b is the bottom layer's reflectance, R_f is the reflectance of the top layer when its optical thickness (d) is infinite, and S is the scattering coefficient of the foreground layer. All of these parameters except for d are dependent on wavelength. For most practical purposes, Sd can be treated as a single quantity. Note that R_f and R_b are conventionally denoted as R_∞ and R_g, respectively; however, for clarity of comparison to related models, we employ our own notation.

The KM model offers some degree of physical accuracy in representing the reflectance of layered surfaces, but is formulated based on certain conditions [15, 4]: the layers contain colorants that scatter and absorb light (optically homogeneous objects are excluded); the layer is flat and infinite; effects of polarization of light are ignored; the layer behaves as if the pigment particles are large with respect to the wavelength of light but very small compared to the thickness of the layer; the layer does not generate light within it; and each layer has uniform optical parameters. While theoretically these constraints should be fulfilled, in practice some constraints can be broken without significantly undermining the accuracy of the estimation. For example, the layer need not be infinite in area for this model to be useful.

Importantly, due to the straightforward computation, the KM model is often used to estimate the mixed reflectance (R_m) from given the values of the parameters (R_f, R_b, Sd). However, to estimate the top layer reflectance (R_f) and the opacity (Sd) from given the values of the mixed reflectance (R_m) and the bottom reflectance (R_b), the problem becomes intractable.

4. Verification

Mudgett *et al*. [19] analyze the accuracy of the KM model by comparing with a multi-flux scattering model, which can be considered as a physically precise model of layered scattering. For various absorption and scattering values, they showed that the KM model is sufficiently correct for media whose scattering coefficient is larger than the absorption coefficient. They concluded that for $K/S < 0.1$, i.e., when scattering is more dominant than absorption, such as in objects with high particle densities, the errors in the KM model are negligible.

Theoretically, considering Eq.(6) and how it is derived, besides the absorption, the KM model explicitly includes two directions of scattering, namely, forward scattering and backward scattering. While in Lambert-Beer law (Eq. (3)), μ is the total attenuation, which represents only the absorption without explicitly involving any scattering [3]. Regarding this difference, it might be concluded that any models based on Lambert-Beer law will fail to be applied to any scattering media.

However, the LB-based model in Eq.(4) is different from the original Lambert-Beer law (Eq.(3)). In the right hand side of the equation, there is an additional energy representing the top layer and the attenuation. With this additional term, we intend to verify the model when it is specifically applied to layered surfaces, by experimentally comparing it with the KM model.

In this paper, in doing the comparisons, first, we calculate the errors between real spectra and simulated spectra of the models for verifying the accuracy of the reflection models (both the KM model and the LB-based model). Second, we calculate the error of the fitting using the spider model.

4.1. Setup

To have accurate measurements, in our experiment we used a spectrometer (Ocean optics's USB2000+) to acquire spectral data of an object attached to an integrating sphere (LabSphere's RSA-FO-150) and halogen light (Ocean optics's LS-1), which can provide the incident light intensity and reduce noise from ambient lights. Fig. 5 shows our experimental setup. As the target objects, we mainly used various watercolors and powder mineral pigments, where the latter were used in wall paintings in Japanese ancient tumuli. Note that, watercolors previously have been shown to follow the KM model [8]. Fig. 6 shows our target substances.

4.2. Procedure

In conducting the comparisons, we are guided the following procedure:

1. We obtain the mixed reflectance (R_m) by canceling the incident light intensity.

2. We estimate the top layer reflectance (R_f) by first calculating the scattering and absorption coefficients (S and K) from totally black and white bottom layers. The calculation is done by using the following equations ([13, 12]):

$$S = \frac{1}{b}\coth^{-1}\left(\frac{b^2-(a-R_w)(a-1)}{b(1-R_w)}\right), \quad (7)$$

where

$$a = \frac{1}{2}\left(R_w - \frac{R_z - R_w + 1}{R_z}\right), \quad (8)$$

$$b = \sqrt{a^2-1}. \quad (9)$$

R_w is the mixed reflectance of the top layer on a totally white bottom layer, and R_z is the mixed reflectance of the top layer on a totally black bottom layer. Having obtained S and a, we can calculate the absorption coefficient by $K = S(a-1)$. Finally, R_f (the top layer reflectance) is calculated by

$$R_f = \left(1 + \frac{K}{S} + \sqrt{\frac{K^2}{S} + 2\frac{K}{S}}\right)^{-1}. \quad (10)$$

Alternatively, R_f can also be measured directly from the substance when the layer is very thick (so thick, that the light cannot penetrate the bottom layer).

3. Having the values of R_b, R_f and S, we can generate synthetic R_m for any thickness d using the KM model. In our experiments, we used a least square method to obtain the appropriate thickness. The generated R_m is then compared with the observed R_m (obtained at Step 1), which is our ground truth.

4. Similarly, from the calculated R_f and observed R_b, we can generate synthetic R_m for any opacity ϕ using the LB-based model. In our experiments, we used a least square method to obtain the appropriate opacity. The generated R_m is also compared with the observed R_m.

4.3. Accuracy of the LB-based Model

We conducted the experiments using ten different watercolors and two powder mineral pigments (Fig. 6). In one of the experiments, we acquired the mixed spectral reflectance

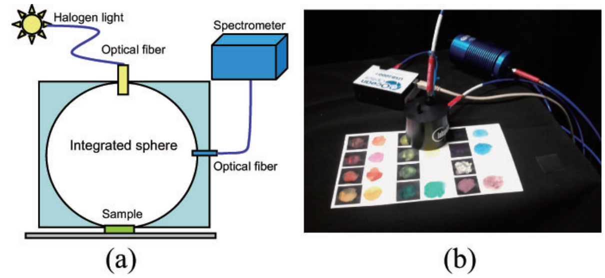

Figure 5. (a) The schematic setup. (b) The real setup.

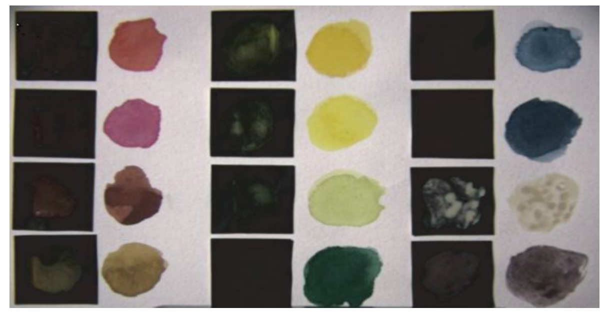

Figure 6. The target substances: watercolors and mineral pigments. The two most bottom of the most right row are the mineral pigments.

of the cobalt blue (the top most right color in Fig. 6), whose spectral reflectance can be observed in Fig. 7.a. The lines in the graph represent different thickness of the watercolor. Fig. 7.b and c show the generated synthetic reflectance using the KM and the LB-based model, respectively. We calculated the sum of the error for every wavelength. The synthetic reflectance generated by the KM model produced a total error of 0.3093, while the LB-based model produced 0.3938. This shows that in the case of the cobalt blue, the LB-based model is sufficiently close to the KM model.

In one of the worst cases (the largest errors), the KM model produced 0.8926, while the LB-based model produced 1.0704. This is the case of the vermilion (the top left most color in Fig. 6). Fig. 8 shows the observed reflectance and the generated ones. The reason for the large error in the LB-based model is because the substance has a relatively large scattering coefficient.

Overall, the errors of all the watercolors and mineral pigments were measured, and shown in Fig. 9. As can be observed in the figure, the error differences between the KM model's and the LB-based model's generated reflectance are relatively small.

4.4. Verification of the Spider Model

To verify the accuracy of the spider model, we followed the following steps:

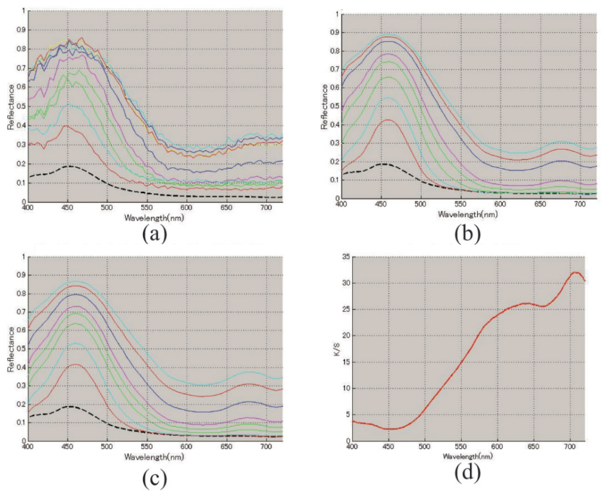

Figure 7. Experiment target: cobalt blue. Top left: the observed spectra of the substance. The various lines represent the spectra at different locations (thickness). The black dash line is the spectra of R_f. Top right: the generated spectra using the KM model. Bottom left: the generated spectra using the LB-based model. Bottom right: The values of K/S.

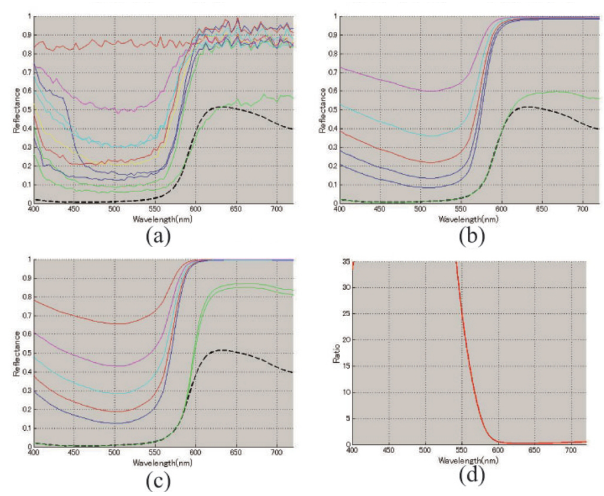

Figure 8. Experiment target: vermilion. Top left: the observed spectra of the substance. The various lines represent the spectra at different locations (thickness). The black dash line is the spectra of R_f. Top right: the generated spectra using the KM model. Bottom left: the generated spectra using the LB-based model. Bottom right: The values of K/S.

1. Using the procedure described in Section 4.2, we generated the synthetic mixed reflection using the KM model and the LB-based model.

2. We chose three values of the spectral reflectance at different wavelengths, representing the peaks of RGB camera sensitivities (440nm, 552nm, 640nm).

3. We generated many mixed reflectance values by changing the thickness.

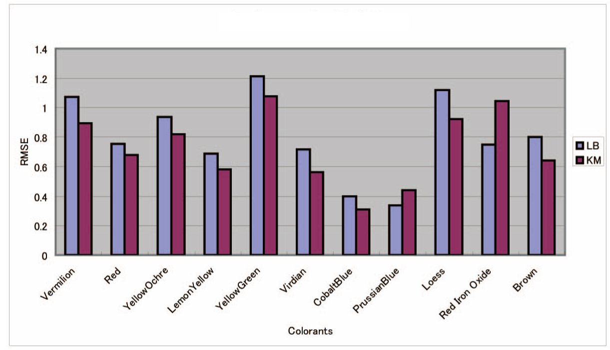

Figure 9. The errors for the simulations of all experiment targets.

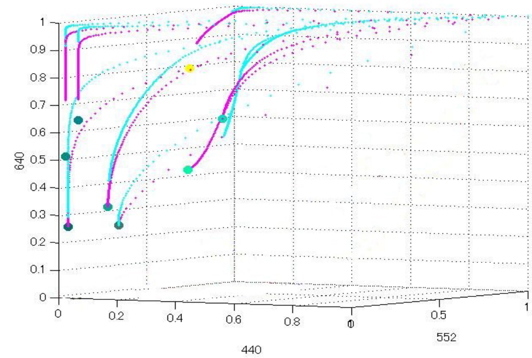

Figure 10. The blue lines represent the LB-based model, and the purple lines represent the KM model. Different lines represent different colors.

4. We projected the mixed reflectance values onto a 3D space, representing the three wavelengths.

Fig. 10 shows the comparison of the lines in the 3D space generated by the KM model and the LB-based model. As can be seen, the generated shapes by the two models are, in most cases, similar.

Aside from projecting the synthetic reflectance, we also verified the distributions of the observed data and the fitting result of the spider model. We expect that if the fitting result is sufficiently close for various colors, then the spider model is reliable in estimating the layered surfaces' parameters. Fig. 11 shows the fitting of all colorants, which represents the success of fitting most of the color lines. Note that, in the figures, there are some location discrepancies between the lines generated by the two models (the yellow and red lines) and the projected points of the pixel intensities (the dark blue points). The reason of this is because, the pixel intensities were acquired by using a digital camera, while the lines were calculated from the spectrometer's data.

5. Discussions

From the experimentation, we can conclude that:

1. We confirm the result of Mudgett *et al*. [20] that when

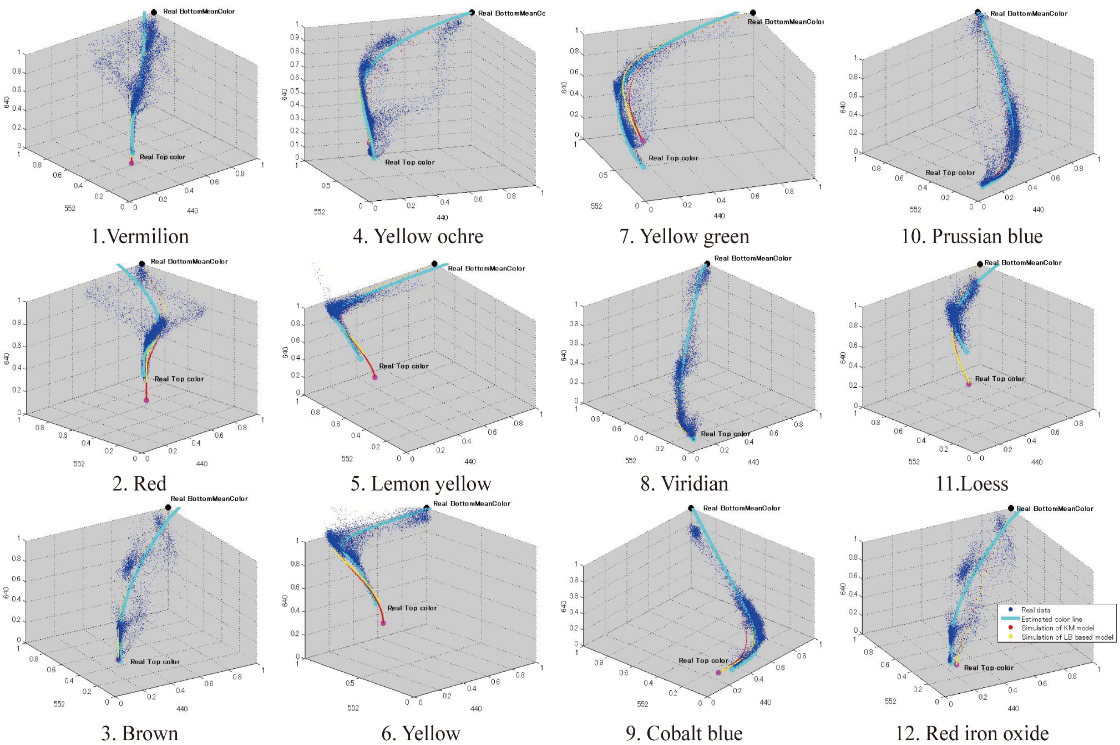

Figure 11. The fitting using spider model.The dark blue points are the projection from the input image taken by a digital camera. The blue lines show the results of fitting by the spider model. The yellow lines show the simulation by the LB-based model. The red lines shows the simulation by the KM model. The yellow and red lines are computed from spectrometer's data.

scattering is more dominant than absorption, the KM model works reliably accurate. This can be observed particularly in Fig. 8.d. Namely, when K/S is considerably small, the synthetic spectra in Fig. 8.b are similar to the observed spectra in Fig. 8.a.

2. From Fig. 7 and Fig. 8, in most cases the LB-based model can generate spectra that are similar to those of the KM model. However, the result in Fig. 8.d shows that the LB-based model can be inaccurate when K/S is considerably small, namely when scattering is more dominant than absorption.

3. Fig. 3.b shows that, in a three-dimensional space (which can be the RGB space), the curves generated by the KM and the LB-based models are similar. This is further shown in Fig. 11, in comparison with the observed data.

4. Fig. 11 shows that the spider model can reliably fit to the observed layered surface data.

5. We confirmed generally the errors of the KM model are less than LB-based model, as shown in Fig. 9.

6. Overall, importantly the errors of the LB-based model are relatively small with respect to those of the KM based model (Fig. 9). Therefore, the LB-based model is comparable to the KM model, however its model is much simpler.

Fig. 12 shows the decomposition result of a few colorants. The result of the estimated values of F for every pixel is shown in Fig. 12.b, which represents the success of the decomposition using the spider model. However, in Fig. 12.b, there are some inaccuracy in the area between color 5 and color 6. This is because their color lines are considerably close (implying the inaccuracy was not caused by the spider model).

6. Conclusion

In this paper, we have verified the LB-based model for layered surfaces from the perspective of the Kubelka-Munk (KM) model, both theoretically and empirically. Besides, we also verified the accuracy of the spider model. We consider our verifications can benefit the progress of layered-surface analysis. Since, by being able to show the LB model and spider model work appropriately for layered surfaces, and to show the conditions where they work, we can have considerable confidence in using the relatively simple models.

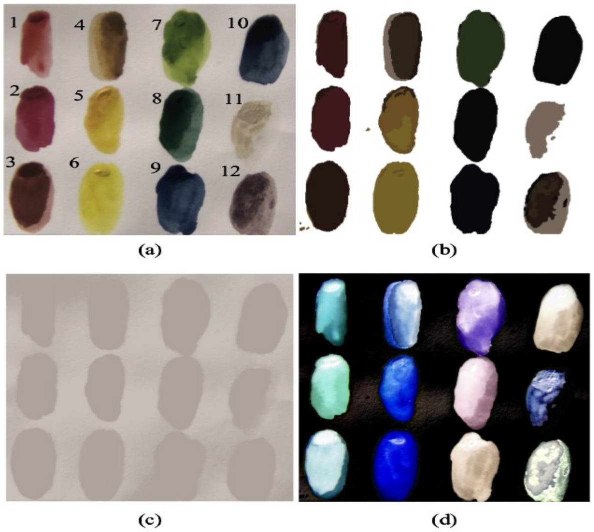

Figure 12. The result of layered surface decompostion. (a) Input image.(b) top layer (c) bottom layer (d) opacity.

7. Acknowledgement

This research is granted by the Japan Society for the Promotion of Science (JSPS) through the "Funding Program for Next Generation World-Leading Researchers (NEXT Program)," initiated by the Council for Science and Technology Policy (CSTP).

References

[1] R.R. Anderson and J.A. Parrish. The optics of human skin. *The Journal of Investigative Dermatology*, 77:13–19, 1981. 1

[2] A. Beer. Bestimmung der absorption des rothen lichts in farbigen flussigkeiten. *Ann. Phys. Chem*, 86(2):78–90, 1852. 2, 3

[3] R.S. Berns. *Principles of color technology*. Wiley Interscience, New York, third edition, 2000. 4

[4] F.W. Billmeyer and R.L. Abrams. Predicting reflectance and color of paint films by kubelka-munk analysis: I. turbid-medium theory. *Journal of Paint Technology*, 45(578):23–30, 1973. 2, 4

[5] M. Born and E. Wolf. *Principles of Optics*. Cambridge, seventh edition, 1999. 2

[6] S. Chandrasekhar. *Radiative Transfer*. Dover, New York, 1960. 2

[7] Y. Chuang, B. Curless, D.H. Salesin, and R. Szeliski. A bayesian approach to digital matting. *in proceeding of IEEE CVPR*, 2001. 2

[8] C. Curtis, S. Anderson, J. Seims, K. Fleischer, and D. Salesin. Computer-generated watercolor. *ACM SIGGRAPH*, 1997. 4

[9] H.R. Davidson and H. Hemmendinger. Color prediction using the two-constant turbid-media theory. *Journal of Optics Society of America*, 56(8):1102–1109, 1966. 2

[10] J. Dorsey and P. Hanrahan. Modelling and rendering of metallic patinas. *In Computer Graphics Processing, ACM SIGGRAPH*, 1996. 2

[11] C.S. Haase and G.W. Meyer. Modeling pigmented materials for realistic image synthesis. *ACM Transactions on Graphics*, 11(4):305–335, 1992. 2

[12] D.B. Judd and G. Wyszecki. *Color in Business, Science and Industry*. John Wiley & Sons, New York, 3rd edition, 1975. 4, 5

[13] G. Kortoum. *Reflectance Spectroscopy*. Springer-Verlag, New York, 1969. 2, 4, 5

[14] H. Koschmieder. Theorie der horizontalen sichtweite. *eitr.Phys. Freien Atm*, 12, 1924. 2

[15] P. Kubelka and F. Munk. Ein beitrag zur optik der farbanstriche. *Z. Tech. Phys*, 12:593–601, 1931. 2, 4

[16] J.H. Lambert. Photometria sive de mensura de gratibus luminis, colorum et umbrae. *Eberhard Klett: Augsberg, Germany*, 1760. 1

[17] A. Levin, D. Lischinski, and Y. Weiss. A closed form solution to natural image matting. *in proceeding of IEEE CVPR*, 2006. 2

[18] T. Morimoto, R. T. Tan, R. Kawakami, and K. Ikeuchi. Estimating optical properties of layered surfaces using the spider model. *in proceeding of IEEE CVPR*, 2010. 1, 2, 3

[19] P.S. Mudgett and L.W. Richard. Multiple scattering calculations for technology. *Applied Optics*, 10(7):1485–1502, 1971. 2, 4

[20] P.S. Mudgett and L.W. Richard. Multiple scattering calculations for technology ii. *Journal of Colloid and Interface Science*, 39(3):551–567, 1972. 2, 6

[21] S. Narasimhan and S.K. Nayar. Interactive deweathering of an image using physical models. *IEEE Workshop on Color and Photometric Method in Computer Vision*, 2003. 2

[22] N. Tsumura, H. Haneishi, and Y. Miyake. Independent-component analysis of skin color image. *JOSA A.*, 16(9):2169–2176, 1999. 2

[23] N. Tsumura, N. Ojima, K. Sato, M. Shiraishi, H. Shimizu, H. Nabeshima, S. Akazaki, K. Hori, and Y. Miyake. Image-based skin color and texture analysis/synthesis by extracting hemoglobin and melanin information in the skin. *ACM SIGGRAPH*, pages 770–779, 2003. 2

[24] G. Wyszecki and W.S. Stiles. *Color Science: Concept and Methods, Quantitative Data and Formulae*. Wiley Inter-Science, second edition, 1982. 4